Journal of Medicinal Chemistry Article

J. Med. Chem. **2009,** *52,* 6599–6605 **6599**
DOI: 10.1021/jm900563e

Antagonists of the Calcium Receptor. 2. Amino Alcohol-Based Parathyroid Hormone Secretagogues

Robert W. Marquis,*[,†] Amparo M. Lago,[†] James F. Callahan,[†] Attiq Rahman,[†] Xiaoyang Dong,[†] George B. Stroup,[‡] Sandra Hoffman,[‡] Maxine Gowen,[‡] Eric G. DelMar,[⊥] Bradford C. Van Wagenen,[⊥] Sarah Logan,[⊥] Scott Shimizu,[⊥] John Fox,[⊥] Edward F. Nemeth,[⊥] Theresa Roethke,[∥] Brian R. Smith,[∥] Keith W. Ward,[∥] and Pradip Bhatnagar[†]

[†]*Departments of Medicinal Chemistry and* [‡]*Bone and Cartilage Biology,* [∥]*Drug Metabolism and Pharmacokinetics, GlaxoSmithKline, 1250 South Collegeville Road, Collegeville, Pennsylvania 19426, and* [⊥]*NPS Pharmaceuticals, 550 Hills Drive, Bedminster, New Jersey 07921*

Received May 6, 2009

When administered as a single agent to rats, the previously reported calcium receptor antagonist **3** elicited a sustained elevation of plasma PTH resulting in no increase in overall bone mineral density. The lack of a bone building effect for analogue **3** was attributed to the large volume of distribution (V_{dss}(rat) = 11 L/kg), producing a protracted plasma PTH profile. Incorporation of a carboxylic acid functionality into the amino alcohol template led to the identification of **12** with a lower volume of distribution (V_{dss}(**12**) = 1.18 L/kg) and a shorter half-life. The zwitterionic nature of antagonist **12** necessitated the utility of an ester prodrug approach to increase overall permeability. Antagonist **12** elicited a rapid and transient increase in circulating levels of PTH following oral dosing of the ester prodrug **11** in the dog. The magnitude and duration of the increases in plasma levels of PTH would be expected to stimulate new bone formation.

Introduction

Osteoporosis is a disease afflicting more than 10 million women and men in the U.S. alone.[1] The overall weakening of bone that results in osteoporosis is caused by a shift in the equilibrium of bone remodeling in which bone formation by osteoblasts is overtaken by the resorption of old bone by osteoclasts. Current treatments to correct this imbalance may be divided into two distinct mechanistic classes. The first class is the antiresorptives which directly inhibit osteoclast activity, thereby slowing the resorption side of the bone remodeling equilibrium. This class is exemplified by bisphosphonates, selective estrogen receptor modulators (SERMs[a]), hormone replacement therapy (HRT), and calcitonin. All of these antiresorptive agents have proven efficacy in humans for the treatment of osteoporosis, slowing the excess resorption of bone but offering little in terms of stimulating the formation of new bone. The second mechanistic class for the treatment of osteoporosis is the bone forming agents which increase osteoblast activity allowing these cells to keep pace with or outperform bone resorbing osteoclasts. Both parathyroid hormone (PTH) (Nycomed) and its N-terminal 1−34 amino acid fragment teriparatide (Lilly),[2] when administered daily by subcutaneous injection, stimulate the formation of new bone, increase bone mineral density, and decrease the risk of fractures.

An alternative approach to the development of an orally active bone forming agent, based upon the clinically validated mechanism of subcutaneously administered osteogenic PTH peptides, would be to identify an agent that would elicit the secretion of endogenously stored parathyroid hormone from the parathyroid glands. Here, the secretion of parathyroid hormone is under the control of the calcium receptor (CaR).[3] This family C G-protein-coupled receptor is capable of sensing minute fluctuations in circulating levels of serum calcium such that a drop in the concentration of calcium levels (hypocalcaemia) elicits the release of PTH from the parathyroid glands while an increase in calcium levels (hypercalcimia) suppresses the release of this hormone. The effects of hypercalcemia can be mimicked by calcimimetic compounds that inhibit the secretion of PTH. One such compound is cinacalcet (**1**, Figure 1),[4] an allosteric activator of the CaR that is used to treat hyperparathyroidism. Calcimimetic compounds validate the view that circulating levels of PTH can be pharmacologically controlled by a small molecule acting at the parathyroid gland CaR. On the other hand, small molecule antagonists of the CaR, known as calcilytics, serve to mimic a hypocalcemic state and elicit the secretion of PTH.[5] If the profile of PTH secretion following antagonism of the CaR is rapid and transient then this should promote the formation of new bone. If however the profile of PTH secretion following antagonism of the receptor is protracted, then this will have an overall catabolic effect and lead ultimately to an undesirable excess resorption of bone. As such, the design of a CaR antagonist capable of promoting overall bone growth is predicated upon this compound's ability to briefly antagonize the receptor, thereby eliciting a transient release of endogenous PTH.[6]

Recently we have reported on the amino alcohol analogue **2** (Figure 1 and Table 1) which was identified as a weak

*To whom correspondence should be addressed. Phone: 1-610-917-7368. Fax: 1-610-917-4206. E-mail Robert.W.Marquis@gsk.com.

[a] Abbreviations: CaR, calcium receptor; PTH, parathyroid hormone; HEK, human embryonic kidney; OVX, ovariectomized; SAR, structure−activity relationship; DAT, dopamine transporter; SERT, serotonin transporter; NET, norepinephrine transporter; CYP2D6, cytochrome P450 2D6; hERG, human ether-a-go-go related gene; FLIPR, fluorimetric imaging plate reader; SERM, selective estrogen receptor modulator; HRT, hormone replacement therapy.

Published on Web 10/12/2009

antagonist of the CaR through a screening effort of the former SmithKline Beecham compound collection.[7] Compound **2** had originally been profiled in a legacy program focused on the discovery of β-adrenergic receptor agonists and antagonists where it was shown to be a potent antagonist of the β_2-adrenergic receptor and an agonist of the β_3-adrenergic receptor. Additionally, **2**, being a lipophilic basic amine and a common pharmacophore for a variety of targets, was also a potent inhibitor of several monoamine transporters, the human ether a-go-go related gene (hERG) ion channel as well as the 2D6 cytochrome P450 (Table 1).[8] Structure−activity studies to optimize the antagonist potency of **2** and to reduce off-target interactions led to the identification of amino alcohol **3** (Figure 1 and Table 1), which is a potent antagonist of the CaR with improved selectivity over the β-adrenergic receptor family. Here, the key selectivity determinant for the CaR compared to β-adrenergic receptors was shown to be the chirality of the secondary hydroxyl group. Although this modification resulted in a significant reduction in affinity for the β-receptor, it did not greatly improve selectivity against the other off-target interactions mentioned above (see Table 1). Despite concerns regarding these off-target interactions, amino alcohol **3** was progressed into an ovariectomized (OVX) rat study to assess its ability to stimulate the formation of new bone.[9] When dosed orally for 8 weeks, analogue **3** elicited a robust but sustained elevation of plasma PTH in the OVX rat. This protracted rise in PTH levels ultimately led to increased bone turnover with no increases in overall bone mineral density. The undesirable PTH profile elicited by analogue **3** was attributed to its prolonged pharmacokinetic profile in the rat where it was shown to be rapidly cleared (Cl = 73.8 (mL/min)/kg) with a large volume of distribution (V_{dss} = 11 L/kg). On the basis of these data, an ideal follow-up to analogue **3** would have a significantly reduced volume of distribution while maintaining the rapid rate of clearance. A molecule with these two characteristics would be expected to have an improved pharmacokinetic profile with a short-lasting antagonism of the CaR, resulting in a transient plasma PTH exposure. In this account we detail structure−activity and pharmacokinetic studies that further address the off-target interactions associated with the amino alcohol class of antagonists as well as the protracted pharmacokinetic profile of analogue **3**.

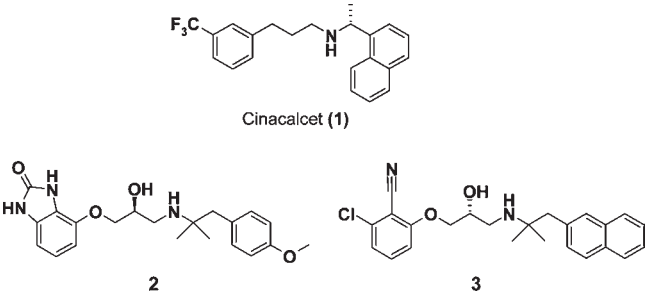

Figure 1. Calcimimetic and calcilytic compounds.

Synthesis Chemistry

The analogues detailed in this account were synthesized according to the reactions provided in Schemes 1−3. Compound **5** of Scheme 1 was synthesized starting with the coupling of 2-cyanophenol (**4**) with (2*R*)-2-oxiranylmethyl 4-nitrobenzenesulfonate to provide the intermediate chiral epoxide (not shown). Opening of this epoxide with [1,1-dimethyl-2-(2-naphthalenyl)ethyl]amine in refluxing ethanol provided **5**. In a similar fashion, as outlined in Scheme 2, alkylation of ethyl 4-hydroxyhydrocinnamate (**6**) with (2*S*)-2-oxiranylmethanol provided the epoxide **7** which was opened with [1,1-dimethyl-2-(2-naphthalenyl)ethyl]amine in refluxing ethanol to provide the ethyl ester **8**. Hydrolysis of **8** under basic conditions gave the acid **9**. Analogues **11** and **12** of Scheme 3 were synthesized beginning with bromination of 4-hydroxyhydrocinnamate (**6**) followed by cyanation and alkylation with (2*S*)-2-oxiranylmethanol to provide epoxide **10**. Opening of epoxide **10** with [1,1-dimethyl-2-(2-naphthalenyl)ethyl]amine provided the ester **11** which was hydrolyzed under basic conditions to give the acid **12**.

Results and Discussion

To assess the ability of synthesized analogues to antagonize the CaR, two in vitro assays were used. The first was a fluorimetric imaging plate reader (FLIPR) based assay measuring the ability of test compounds to block increases in the concentration of cytoplasmic Ca^{2+} in HEK293 cells expressing the human parathyroid CaR. The second was a binding assay where analogues were tested for their ability to displace the tritiated calcimimetic radioligand (2-(2-hydroxyphenyl)-6-methyl-5-(2-methylpropyl)-3-(2-phenylethyl)-4(3*H*)-pyrimidinone) from membrane preparations of HEK293 cells expressing the human CaR. The hydrochloride salts of the synthesized compounds were prepared in order to facilitate both compound solubility and handling.

As detailed previously analogue **3** is a potent antagonist of the CaR in both the binding assay and the FLIPR assay with

Scheme 1. Synthesis of Antagonist **5**[a]

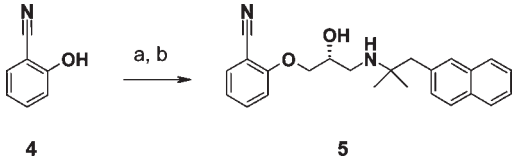

[a] Reagents and conditions: (a) NaH, DMF, (2*R*)-2-oxiranylmethyl 4-nitrobenzenesulfonate, 0 °C; (b) [1,1-dimethyl-2-(2-naphthalenyl)ethyl]-amine, EtOH, 70 °C.

Table 1. Potency and Selectivity Data[a]

	IC$_{50}$ (μM)							
compd	CaR FLIPR	CaR binding	SERT binding	NET binding	DAT binding	CYP2D6	hERG Bbinding	β_2 binding
2	11.0	31.8	0.061	0.60	1.20	1.26	11.8	0.0013
3	0.058	0.003	0.002	0.20	0.20	0.045	3.00	4.3
5	0.018	0.003	0.003	0.003	0.002	0.100	3.20	ND
9	>25	4.8	0.068	16.0	3.7	52.0	38.5	>30.0
11	0.034	0.003	0.078	0.037	0.059	3.0	1.7	14.0
12	0.200	0.022	0.023	5.40	2.80	>50.0	32.7	>30.0

[a] IC$_{50}$ values represent the average of at least three individual titrations. ND = not determined.

Scheme 2. Synthesis of Antagonists **8** and **9**[a]

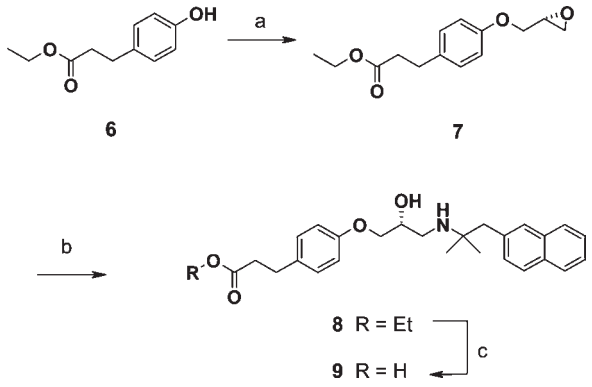

[a] Reagents and conditions: (a) DIAD, PPh_3, (2*S*)-2-oxiranylmethanol, THF, 0 °C to room temp; (b) [1,1-dimethyl-2-(2-naphthalenyl)ethyl]-amine, EtOH, 70 °C; (c) NaOH, EtOH, H_2O.

Scheme 3. Synthesis of Antagonists **11** and **12**[a]

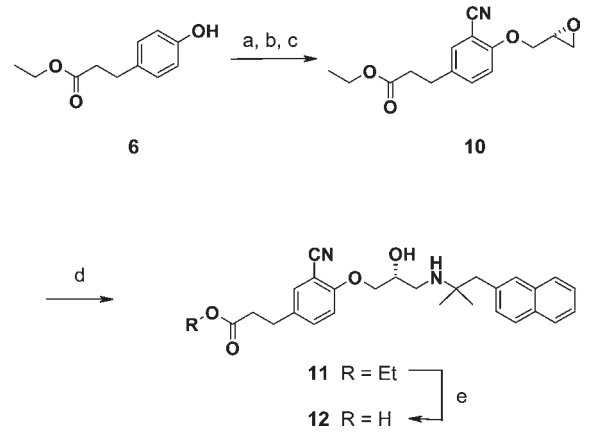

[a] Reagents and conditions: (a) Br_2, $CHCl_3$, 0 °C; (b) CuCN, NMP, reflux; (c) DIAD, PPh_3, (2*S*)-2-oxiranylmethanol, THF, 0 °C to room temp; (d) [1,1-dimethyl-2-(2-naphthalenyl)ethyl]amine, EtOH, 70 °C; (e) CH_3OH, 3 N NaOH.

IC_{50} values of 0.003 and 0.058 μM, respectively (Table 1). This potency represents a greater than 10000-fold increase in potency in the CaR binding assay and a 190-fold increase in potency in the functional assay over the original lead **2**. In a binding assay format, analogue **3** is also a potent inhibitor of the serotonin, norepinepherine, and dopamine transporters with IC_{50} values of 0.002, 0.200, and 0.200 μM, respectively, as well as both the 2D6 cytochrome P450 (IC_{50} = 0.045 μM) and the hERG ion channel (IC_{50} = 3.00 μM). Importantly, the affinity of **3** for the β_2-adrenergic receptor was reduced almost 3300-fold relative to **2**. Analogue **5**, in which the chlorine atom of **3** was removed, was also a potent antagonist of the CaR with IC_{50} values of 0.003 and 0.018 μM in the binding and functional assays, respectively. Not unexpectedly, this modification did not greatly affect the off-target interactions observed within analogues of this series of antagonists, and as such, this analogue was not further profiled in pharmacokinetic studies. However, this modification did indicate that potent antagonism of the CaR was achievable with the incorporation of a benzonitrile moiety. Incorporation of a propionic acid on the aromatic group to provide analogue **9** resulted in a significant loss in antagonist potency. This result is consistent with structure−activity trends defined earlier within this series in which an electron withdrawing moiety on this aromatic group was found to be required for potent antagonism of the CaR. Despite the lack of CaR antagonist potency for analogue **9**, what was most encouraging was the substantial increase in selectivity for the majority of the off-target interactions characteristic of this amino alcohol series. Similar to previous analogues, **9** remained a potent inhibitor of the serotonin transporter with IC_{50} = 0.068 μM, however, a substantive reduction in potency versus the norepinephrine and dopamine transporters was seen relative to analogues **3** and **5**. Additionally, incorporation of the propionic acid moiety also led to a reduction in activity versus the 2D6 cytochrome P450 isozyme (IC_{50} = 52 μM), the hERG ion channel (IC_{50} = 38.5 μM), and the β_2-adrenoreceptor (IC_{50} > 30 μM). Pharmacokinetic analysis in the rat revealed that **9** had a high rate of clearance (Cl = 117.5 (mL/min)/kg) with a low volume of distribution (V_{dss} = 2.1 L/kg), a short half-life ($T_{1/2}$ = 0.4 h), and mean residence time (MRT = 0.3 h). As discussed above, this type of pharmacokinetic profile was desirable for eliciting a rapid and transient release of PTH. Unfortunately the oral bioavailbilty of **9** was low (approximately 4%), which was likely a reflection of both the high clearance and the low intestinal absorption attributable to the zwitterionic nature of this compound.

Although analogue **9** was not a potent antagonist of the CaR its improved receptor selectivity and desirable intravenous pharmacokinetic profile made this analogue the focus of additional studies aimed at improving both potency and bioavailability. As discussed above, structure−activity studies had revealed that the incorporation of an electron withdrawing moiety on this aromatic group was deemed essential for antagonist potency. Incorporation of the propionic acid side chain of **9** on the aromatic group of the potent antagonist **5** led to analogue **12**, which was a potent antagonist of the CaR with IC_{50} = 0.022 μM in the receptor binding assay and IC_{50} = 0.20 μM in the FLIPR assay. Despite the improved potency versus the CaR, no significant improvement in selectivity for **12** against the serotonin transporter (SERT IC_{50} = 0.023 μM) was observed while improved selectivity over the norepinepherine (NET IC_{50} = 5.40 μM) and dopamine transporters (DAT IC_{50} = 2.80 μM) was observed relative to analogue **3** (SERT IC_{50} = 0.002 μM; NET IC_{50} = 0.002 μM, DAT IC_{50} = 0.20 μM). Incorporation of the propionic acid moiety also led to a significant increase in selectivity of **12** versus CYP2D6 (IC_{50} > 50.0 μM), the hERG ion channel (IC_{50} = 32.7 μM), and the β_2-adrenoreceptor (IC_{50} > 30.0 μM).

Pharmacokinetic analysis of **12** in the rat showed this compound to have a desirable profile with a short half-life ($T_{1/2}$ = 0.56 h), lower mean residence time (MRT = 0.32 h), rapid clearance (Cl = 63.6 mL/min/kg), and low volume of distribution (V_{dss} = 1.18 L/kg). Analogue **12** had a low oral bioavailability (approximately 0.3%) when administered orally as a suspension (48 mg/kg). Dosing into the portal vein of the rat revealed that the first pass hepatic extraction of **12** was moderate to high at 68 ± 21%, suggesting that it is likely a combination of poor intestinal absorption and high first pass hepatic extraction that is limiting the systemic exposure of **12** in the rat following oral administration. Evaluation of the pharmacokinetics of **12** in the dog revealed that this compound had a short half-life ($T_{1/2}$ = 1.23 h) and mean residence time (MRT = 0.85 h) with a small volume of distribution (V_{dss} = 0.78 L/kg) and a moderate rate of clearance (Cl = 15.4 (mL/min)/kg). As was observed in the rat, the rate of first pass hepatic extraction of **12** was high in the dog (90 ± 6%) following intraportal administration. The oral bioavailability

Table 2. Pharmacokinetic Data for Antagonists **3**, **9**, **11**, and **12**[a]

		pharmacokinetics				
compd	species	MRT (h)	$T_{1/2}$ (h)	Cl ((mL/min)/kg)	V_{dss} (L/kg)	F(%)
3	rat	2.5	2.1	73.8	11.03	11.4
9	rat	0.3	0.4	117.5	2.1	4.0
11	rat	0.7	0.88			9.5[b]
11	dog	1.37	1.23			9.1[b]
12	rat	0.32	0.56	63.6	1.18	0.29
12	dog	0.85	1.23	15.4	0.78	ND

[a] Three rats or dogs were employed for the po and iv arms of these studies. ND = not determined. [b] Oral bioavailability of acid **12** following oral dosing of ester **11**.

of **12** in the dog was not determined in these studies because of the low levels of intestinal absorption and high hepatic extraction, similar to what had been previously observed in the rat.

The systemic exposure of **12** in the rat and the dog was limited by two factors: high hepatic extraction and poor intestinal absorption following oral administration. The high hepatic extraction of **12** is likely a required characteristic of a compound that by necessity has to be cleared rapidly in order to limit systemic exposure and antagonize briefly the CaR. Alternatively, in order to address the poor intestinal absorption of **12**, a classic ester prodrug strategy was employed. The ethyl ester prodrug **11** of the parent acid **12** was a potent antagonist of the CaR with an IC_{50} of 0.003 and 0.034 μM in binding and functional assays, respectively (Table 1). Not unexpectedly, the gains in receptor selectivity realized with the parent acid **12** were virtually abolished with the ester prodrug **11**, a likely reflection of this compound's greater lipophilicity (clogP(**11**) = 5.1 versus clogP(**12**) = 2.0) and cell permeability. This loss of target selectivity was of nominal concern because of the well precedented rates of ester prodrug hydrolysis which would lead to the generation of the significantly more selective parent acid **12** in the systemic circulation. Data were therefore gathered in an effort to assess the rates of this transformation in vivo.

In the rat, the oral bioavailability of the parent acid **12** following dosing of a suspension of the ester prodrug **11** (4.7 mg/kg in 1% methylcellulose) was 9.5%, representing a 32-fold increase in exposure when compared to the dosing of a solution of the parent acid **12** (48 mg/kg) (Table 2). None of the ester **11** was detectable in the systemic circulation, indicating complete hydrolysis to the parent acid **12** at this dose. Following intravenous administration, the fractional conversion of the ester **11** to the acid **12** had an apparent half-life of approximately 7 min. Additionally, none of the ester prodrug **11** was observed in the systemic circulation following intraportal infusion (1.8 mg/kg), indicating rapid hydrolysis and/or high hepatic extraction of this compound. A high dose study in the rat (47.5 mg/kg po) conducted to support safety assessment studies revealed that systemic exposure to the ester **11** was very low with maximum blood concentrations of 15−20 ng/mL, again indicative of rapid ester hydrolysis. In the dog, the oral bioavailability of the acid **12** was 9.1% following oral suspension dosing of the ester **11**. In this species the parent acid had a desired short half-life ($T_{1/2}$ = 1.23 h) and mean residence time (MRT = 1.37 h) following the oral administration of a suspension dose of the ester **11**, suggesting rapid dissolution and absorption. The half-life of the ester **11** was estimated to be approximately 7 min with rapid conversion to the parent acid **12** following intravenous administration. Portal vein concentrations indicated that the ester **11** was well absorbed across the intestinal wall and that the acid **12** comprised the majority of the total portal vein AUC (73%). Combined, these data indicate that it is again high first pass hepatic extraction, not poor absorption, limiting the bioavailability of the parent acid **12** following the oral administration of the ester **11** in these two species.

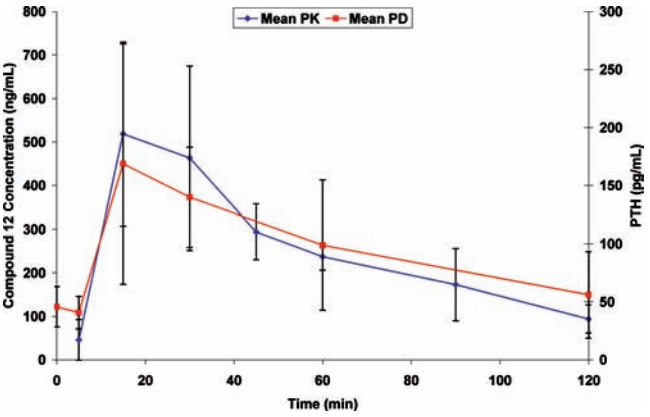

Figure 2. Mean pharmacokinetics and pharmacodynamics of analogue **12** following the oral dosing of a 23.4 mg/kg suspension dose (1% methylcellulose) of **11** in the dog (n = 3).

The promising pharmacokinetic profile of the potent acid **12** following oral dosing of the ester prodrug **11** prompted evaluation of this acid/ester prodrug pair for its ability to elicit an increase in plasma levels of PTH in the dog. As shown in Figure 2, oral administration of the ester **11** (23.4 mg/kg) produced a rapid increase of the parent acid **12** in the systemic circulation with an oral T_{max} of 0.5 h and an oral C_{max} of 597 ng/mL. This profile suggests that the ester **11** rapidly dissolved in intestinal fluid, was well absorbed across the intestinal wall, and was completely converted to the parent acid **12** via ester hydrolysis. Levels of the acid **12** returned to baseline in approximately 2 h, consistent with the desired profile for brief antagonism of the CaR (Figure 2). A concomitant rise in plasma PTH levels was also observed following the oral dosing of the ester **11**. Plasma PTH levels reached T_{max} at 0.4 h with a C_{max} of approximately 180 ng/mL, a pharmacokinetic profile essentially overlaying that of the acid **12**.

Conclusions

In this account we have detailed structure−activity studies focused on the improvement of both the in vitro selectivity and in vivo pharmacokinetic profiles of the first generation amino alcohol-based CaR antagonist **3**. The incorporation of a polar carboxylic acid moiety into this template to provide analogue **12** served the dual purposes of improving both the CaR selectivity and pharmacokinetic profiles of **3**. However, because of the high first pass hepatic extraction and low intestinal absorption, the oral bioavailability of **12** was low, prompting the use of an acid/ester prodrug strategy. The ester **11** was able to deliver significant levels of the acid following oral administration in both the dog and the rat and maintained a desired short exposure profile. Oral administration of the ester **11** in the dog elicited a rapid and transient increase in plasma levels of PTH. The magnitude and duration of the increases in plasma levels of PTH would be expected to stimulate new bone formation. This pharmacokinetic profile represents a significant improvement over the first generation antagonist **3**. The ability of analogues such as **12** to promote a bone building effect in vivo will be the subject of a future publication.

Experimental Procedures

Calcium Receptor Inhibitor Assay. HEK 293 4.0-7 cells were constructed as described by Rogers et al. (*J. Bone Miner. Res.* **1995**, *10* (Suppl. 1), S483). At 48 h prior to running the CaR assay, frozen HEK293 CaRec4.0-c17 cells are thawed, counted, and diluted to 3×10^5/mL (15K/50 μL). The cell medium used to dilute the cells consists of 1:1 DMEM/F12 (HAM'S) with L-glutamine, 15 mM HEPES, phenol red, 10% fetal bovine serum, and 1% penicillin−streptomycin solution. Cell solution is seeded at (15K cells/50 μL)/well in Greiner poly-D-lysine coated 38-well, black, clear-bottom tissue culture plates and left at room temperature for 1 h to reduce the edge effect. After the first hour at room temperature, cell plates are then placed into a 37 °C, 5% CO_2 incubator for 48 h.

On the day of the experiment, plate confluency is first checked via microscope. Wells should be ~100% confluent in an even cell monolayer. Assay reagents are prepared fresh. Dye load buffer consists of Hank's buffered saline solution with 0.75 mM calcium, without magnesium, without sodium bicarbonate, with 20 mM Hepes, probenecid (2.5 mM final concentration), Fluo4 (2 μM final concentration), and Brilliant Black (500 μM final concentration). Compound dilution buffer consists of Hank's buffered saline solution without calcium, without magnesium (without sodium bicarbonate), and with CHAPS (0.01% final concentration). A ligand curve plate is also prepared fresh. A 16 point curve is dispensed into a Greiner 384-well polypropylene plate. The top concentration of the ligand, CaCl, is 2.875 mM (final concentration), and the lowest concentration is 0.375 mM (final concentration). An EC_{80} value is generated from the curve data.

The CaR assay begins when the cell medium is aspirated from the cell plate using a Tecan plate washer, leaving nothing but the cell monolayer. Dye load buffer is added to the cell plate at 20 μL/well using a Multidrop, and the loaded plate is incubated for 45 min at 37 °C, 5% CO_2. Compound plates are received with 1 μL of compound stamped at 5 mM top concentration (25 μM final concentration in cell plate). Compound dilution buffer is added to columns 1−24 in the compound plate at 65 μL/well using a Multidrop. Column 6 is prestamped with 1 μL of DMSO to represent the high control, and column 18 receives 65 μL of buffer as the low control. The compound addition takes place on a Cybi Well dispenser when 10 μL of diluted compound is added to the dye loaded cell plate. The cell plate with compound is then incubated at room temperature for 5 min. The antagonist addition takes place on the FLIPR when 10 μL of EC_{80} challenge is added to the cell plate and fluorescence imaging proceeds for 65 s. Column 18 of the EC_{80} challenge plate contains only buffer to represent a low control or tool antagonist.

Calcium Receptor Binding Assay. HEK 293 4.0-7 cells stably transfected with the human parathyroid calcium receptor ("HuPCaR") were scaled up in T180 tissue culture flasks. Plasma membrane is obtained by Polytron homogenization or glass douncing in buffer (50 mM Tris-HCl, pH 7.4, 1 mM EDTA, 3 mM $MgCl_2$) in the presence of a protease inhibitor cocktail containing 1 μM leupeptin, 0.04 μM pepstatin, and 1 mM PMSF. Aliquoted membrane was snap frozen and stored at −80 °C. ^{3}H labeled compound was radiolabeled to a radiospecific activity of 44 Ci/mmol and was aliquoted and stored in liquid nitrogen for radiochemical stability.

A typical reaction mixture contains 2 nM ^{3}H compound ((*R*, *R*)-*N*-4′-methoxy-*t*-3-3′-methyl-1′-ethylphenyl-1-(1-naphthyl)-ethylamine) or ^{3}H compound ((*R*)-*N*-[2-hydroxy-3-(3-chloro-2-cyanophenoxy)propyl]-1,1-dimethyl-2-(4-methoxyphenyl)ethylamine) and 4−10 μg of membrane in homogenization buffer containing 0.1% gelatin and 10% EtOH in a reaction volume of 0.5 mL. Incubation is performed in 12 × 75 polyethylene tubes in an ice−water bath. To each tube 25 μL of test sample in 100% EtOH is added, followed by 400 μL of cold incubation buffer and 25 μL of 40 nM ^{3}H-compound in 100% EtOH for a final concentration of 2 nM. The binding reaction is initiated by the addition of 50 μL of 80−200 μg/mL HEK 293 4.0-7 membrane diluted in incubation buffer, and the mixture is allowed to incubate at 4 °C for 30 min. Wash buffer is 50 mM Tris-HCl containing 0.1% PEI. Nonspecific binding is determined by the addition of 100-fold excess of unlabeled homologous ligand and is generally 20% of total binding. The binding reaction is terminated by rapid filtration onto 1% PEI pretreated GF/C filters using a Brandel harvestor. Filters are placed in scintillation fluid, and radioactivity is assessed by liquid scintillation counting.

The purities of all tested compounds that were not analyzed via elemental analysis were determined by high performance liquid chromatography. Method A was performed on a Agilent 1100 series, with a UV detector monitoring at 254 nm, a Zorbax SB-C8 column (4.6 mm × 150 mm, 5 μm), 5−100% CH_3CN/H_2O (with 0.02% TFA) over 12.5 min and hold for 2.5 min, and flow rate of 1.5 mL/min at 40°C. Method B was performed on a Agilent 1200 series, with a UV detector monitoring at 254 nm, a Phenomenex C18 column (4.6 mm × 150 mm, 3 μm), 5−95% CH_3CN/H_2O (with 0.1% TFA) over 15 min, and flow rate of 1 mL/min at 40 °C. Method C was performed on an Agilent 1200 series, with a UV detector monitoring at 254/214 nm, a Zorbax-XDB-C18 column (4.6 mm × 75 mm, 3.5 μm), 5−95% CH_3CN/H_2O (each with 0.10 % TFA) over 4 min and hold for 1 minute at 95 % of CH_3CN (0.10% TFA), and flow rate of 2.0 mL/min. All compounds analyzed by these methods possessed purities equal to or greater than 95% with the exception of analogue **5**, which was 95.5% pure by method A and 94.9% pure by method B.

General. Except where indicated materials and reagents were used as supplied. Nuclear magnetic resonance spectra were recorded at either 250 or 400 MHz using, respectively, a Bruker AM 250 or Bruker AC 400 spectrometer. Mass spectra were taken on a PE Syx API III instrument using electrospray (ES) ionization techniques. Elemental analyses were obtained using a Perkin-Elmer 240C elemental analyzer. Reactions were monitored by TLC analysis using Analtech silica gel GF or E. Merck silica gel 60 F-254 thin layer plates. Flash chromatography was carried out on E. Merck Kieselgel 60 (230−400 mesh) silica gel. The purity of all tested compounds, which were not analyzed via elemental analysis, were determined by high performance liquid chromatography. Method A was performed on an Agilent 1100 series, with a UV detector monitoring at 254 nm, a Zorbax SB-C8 column (4.6 mm × 150 mm, 5 μm), 5−100% CH_3CN/H_2O (with 0.02% TFA) over 12.5 min and hold for 2.5 min, and flow rate of 1.5 mL/min at 40 °C. Method B was performed on a Agilent 1200 series, with a UV detector monitoring at 254 nm, a Phenomenex C18 column (4.6 mm × 150 mm, 3 μm), 5−95% CH_3CN/H_2O (with 0.1% TFA) over 15 min, and flow rate of 1 mL/min at 40 °C.

2-[((2*R*)-3-{[1,1-Dimethyl-2-(2-naphthalenyl)ethyl]amino}-2-hydroxypropyl)oxy]benzonitrile (5). To a solution of (2*S*)-glycidol (2 g, 27 mmol) in dichloromethane (25 mL) at 0 °C was slowly added triethylamine (3.75 mL). Then a solution of 4-nitrobenzenesulfonyl chloride (6 g, 27 mmol) in dichloromethane (13 mL) was added to the reaction mixture at such a rate that the temperature did not rise above 15 °C. After 1 h at 0 °C the solution was allowed to warm to room temperature and maintained at this temperature overnight. The reaction mixture was concentrated and the crude material purified by flash column chromatography (0−60% EtOAc/hexane) to afford 4.2 g of the desired product (58%). MS (*m*/*z*): 260.1 (M+H).

Sodium hydride (70 mg, 1.76 mmol, 60% oil suspension) was washed twice with hexane and then placed in a two-necked round-bottom flask under N_2 and cooled to 0 °C with an ice−water bath. Then DMF (5 mL), 2-hydroxybenzonitrile (190 mg, 1.6 mmol), and (2*R*)-2-oxiranylmethyl 4-nitrobenzenesulfonate (500 mg, 1.92 mmol) were added to this mixture. The solution was maintained at 0 °C for 6 h, whereupon it was concentrated

and the crude material was purified by flash column chromatography (0−80% EtOAc/hexane) to afford 240 mg of the 2-{[(2*R*)-2-oxiranylmethyl]oxy}benzonitrile (86%).

A solution of 2-{[(2*R*)-2-oxiranylmethyl]oxy}benzonitrile (239 mg, 1.37 mmol) and 2-methyl-1-(2-naphthalenyl)-2-propanamine (327 mg, 1.64 mmol) in ethanol (10 mL) were combined and heated at 70 °C for 16 h. The mixture was concentrated and purified by column chromatography (0−10% CH_2Cl_2/MeOH) and afforded the desired product (272 mg, 53.2%). This material was dissolved in CH_2Cl_2, and HCl in ether was added. This material was concentrated and azeotropically dried with toluene to provide the hydrochloride salt **5**. ^{1}H NMR (DMSO, 400 MHz): δ 8.95 (m, 1H), 8.72 (m, 1H), 7.08−7.90 (m, 11H), 6.05 (m, 1H), 4.15−4.40 (m, 3H), 3.31−3.46 (m, 1H), 3.15−3.20 (m, 3H), 1.30 (s, 6H). MS (*m*/*z*): 375.3 (M + H). HPLC purities: method A, 95.5%, t_R = 7.2 min; method B, 94.9%, t_R = 8.9 min.

3-{4-[((2*R*)-3-{[1,1-Dimethyl-2-(2-naphthalenyl)ethyl]amino}-2-hydroxypropyl)oxy]phenyl}propanoic Acid (8). To a solution of ethyl 3-(4-hydroxyphenyl)propanoate (**6**, 5.0 g, 25.8 mmol) in 100 mL of THF was added (2*S*)-2-oxiranylmethanol (2.48 g, 33.5 mmol) and triphenylphosphine (10.2 g, 38.7 mmol). The reaction mixture was cooled to 0 °C, and DIAD (8.10 g, 38.7 mmol) was added dropwise. The mixture was allowed to warm to room temperature and maintained at this temperature overnight. A white precipitate formed upon addition with Et_2O and was filtered off through a fine fritted funnel. The filtrate was concentrated and purified by column chromatography to give 4.8 g (75%) of ethyl 3-(4-{[(2*R*)-2-oxiranylmethyl]oxy}phenyl)propanoate (**7**).

A solution of ethyl 3-(4-{[(2*R*)-2-oxiranylmethyl]oxy}phenyl)-propanoate (1.2 g, 4.8 mmol) and [1,1-dimethyl-2-(2-naphthalenyl)ethyl]amine (1.0 g, 5.0 mmol) in ethanol (10 mL) was combined and heated at 70 °C for 15 h. The mixture was concentrated and purified by column chromatography (0−90% ethyl acetate/hexane) and afforded ethyl 3-{4-[((2*R*)-3-{[1,1-dimethyl-2-(2-naphthalenyl)ethyl]amino}-2-hydroxypropyl)oxy]phenyl}propanoate (**8**, 1.4 g, 78%). ^{1}H NMR (400 MHz, $CDCl_3$): δ 9.41 (br, 1 1 H), 8.82 (br, 1 H), 7.91 (m, 3 H), 7.52 (s, 1 H), 7.50 (m, 2 H), 7.40 (d, 1 H, *J* = 8.4 Hz), 7.15 (d, 2 H, *J* = 8.4 Hz), 6.89 (d, 2 H, *J* = 8.8 Hz), 5.95 (d, 1 H, *J* = 4.8 Hz), 4.28 (m, 1 H), 4.03 (m, 4 H), 3.21−3.09 (m, 4 H), 2.79 (t, 2 H, *J* = 7.6 Hz), 2.57 (t, 2 H, *J* = 7.6 Hz), 1.30 (s, 6 H), 1.15(t, *J* = 7.2 Hz). MS(*m*/*z*): 450.2 (M+H). Anal. Calcd for $C_{28}H_{35}NO_4 \cdot$HCl: C 69.19; H 7.46; N 2.88. Found: C 69.14; H 7.44; N 2.83.

3-{4-[((2*R*)-3-{[1,1-Dimethyl-2-(2-naphthalenyl)ethyl]amino}-2-hydroxypropyl)oxy]phenyl}propanoic Acid (9). Sodium hydroxide (3 N, 1.0 mL, 3.0 mmol) was added to a solution of ethyl 3-{4-[((2*R*)-3-{[1,1-dimethyl-2-(2-naphthalenyl)ethyl]amino}-2-hydroxypropyl)oxy]phenyl}propanoate (**8**, 0.50 g, 1.0 mmol) in methanol (15 mL). The mixture was maintained at room temperature for 15 h. The methanol was removed in vacuo, and the aqueous layer was diluted with water. The pH of the aqueous layer was adjusted to pH ∼6.0 with 6 N HCl while stirring. The precipitated white solid was collected by filtration and dried under high vacuum in the oven (∼55 °C) for ∼ 20 h. The zwitterion was taken up in acetonitrile, and 1 N HCl in ether was added and stirred for ∼2 h and then concentrated in vacuo to afford 3-{4-[((2*R*)-3-{[1,1-dimethyl-2-(2-naphthalenyl)ethyl]-amino}-2-hydroxypropyl)oxy]phenyl}propanoic acid (**9**, 0.4 g, 84%) as white foam solid. ^{1}H NMR (400 MHz, $CDCl_3$): δ 11.8 (s, 1 H), 9.41 (br, 1H), 8.85 (br, 1 H), 7.91 (m, 3 H), 7.78 (s, 1 H), 7.51 (m, 2 H), 7.40 (m, 1 H), 7.15 (d, 2 H, *J* = 8.4 Hz), 6.89 (d, 2 H, *J* = 8.4 Hz), 5.96 (d, 1 H, *J* = 4.4 Hz), 4.30 (m, 1 H), 4.02 (d, 2 H, *J* = 5.2 Hz), 3.23−3.03 (m, 4 H), 2.76 (t, 2 H, *J* = 7.6 Hz), 2.50 (t, 2 H, *J* = 7.6 Hz), 1.30 (s, 6 H). MS (*m*/*z*): 422.2 (M+H). Anal. Calcd for $C_{26}H_{31}NO_4 \cdot$HCl: C 68.18; H 6.61; N 2.98. Found: C 68.06; H 7.04; N 3.06

Ethyl 3-{3-Cyano-4-[((2*R*)-3-{[1,1-dimethyl-2-(2-naphthalenyl)-ethyl]amino}-2-hydroxypropyl)oxy]phenyl}propanoate Hydrochloride (11). To a solution of ethyl 3-(4-hydroxyphenyl)propanoate (3.30 g, 17.01 mmol) in chloroform (30 mL) cooled in an ice bath was slowly added bromine (2.85 g, 17.86 mmol) over 25 min. The solution was stirred for 60 min at room temperature and then quenched with water and washed with brine. The organic layer was dried over Na_2SO_4, filtered, concentrated in vacuo, and purified by flash chromatography (Biotage, 0−20% EtOAc/hexanes) to yield ethyl 3-(3-bromo-4-hydroxyphenyl)propanoate (3.54 g, 76%). ^{1}H NMR (400 MHz, $CDCl_3$): δ 1.26 (t, *J* = 7.07 Hz, 3 H), 2.56−2.63 (t, *J* = 7.6 Hz, 2 H), 2.88 (t, *J* = 7.71 Hz, 2 H), 4.11−4.19 (q, *J* = 7.2 Hz, 2 H), 6.95 (d, *J* = 8.34 Hz, 1 H), 7.07 (dd, *J* = 8.34, 2.02 Hz, 1 H), 7.33 (d, *J* = 2.27 Hz, 1 H).

To a solution of ethyl 3-(3-bromo-4-hydroxyphenyl)propanoate (3.54 g, 12.97 mmol) in NMP (20 mL) was added CuCN (1.22 g, 13.62 mmol), and the mixture was refluxed for 2 h. The reaction mixture was cooled to room temperature, diluted with ethyl acetate (70 mL), and then washed with 1 N HCl (60 mL × 2) and brine (60 mL). The organic layer was dried over Na_2SO_4, filtered, concentrated in vacuo, and purified by flash chromatography (Biotage, 10−28%, EtOAc/hexanes) to yield ethyl 3-(3-cyano-4-hydroxyphenyl)propanoate (2.1 g, 73.8%). LCMS (*m*/*z*): 220.0 $[M+H]^+$.

To a solution of ethyl 3-(3-cyano-4-hydroxyphenyl)propanoate (1.95 g, 8.90 mmol) in dry THF (15 mL) was added in sequence (*S*)-glycidol (1.32 g, 17.81 mmol) and PPh_3 (4.67 g, 17.81). The mixture was cooled in an ice bath, and DIAD (4.67 g, 17.81 mmol) was added dropwise. After 20 h, an additional 0.65 equiv of (*S*)-glycidol, PPh_3, and DIAD was added and the mixture was stirred for 3 h at room temperature. The solvent was then evaporated and the residue was purified by flash chromatography (Biotage, 0−1.2% THF/CH_2Cl_2) to yield ethyl 3-(3-cyano-4-{[(2*R*)-2-oxiranylmethyl]oxy}phenyl)propanoate (1.40 g, 57%). MS (*m*/*z*): 294.2 $[M+18]^+$.

To a solution of ethyl 3-(3-cyano-4-{[(2*R*)-2-oxiranylmethyl]-oxy}phenyl) propanoate (0.627 g, 2.3 mmol) in ethanol (10 mL) was added [1,1-dimethyl-2-(2-naphthalenyl)ethyl]amine (0.571 g, 2.87 mmol), and the mixture was stirred at 70 °C for 20 h. The solvent was evaporated, and the residue was purified by flash chromatography (Biotage, 0−3.2% MeOH/CH_2Cl_2) to yield ethyl 3-{3-cyano-4-[((2*R*)-3-{[1,1-dimethyl-2-(2-naphthalenyl)-ethyl]amino}-2-hydroxypropyl)oxy]phenyl}propanoate (0.89 g, 82%). To a solution of ethyl 3-{3-cyano-4-[((2*R*)-3-{[1,1-dimethyl-2-(2-naphthalenyl)ethyl]amino}-2-hydroxypropyl)oxy]-phenyl}propanoate (202 mg, 0.426 mmol) in acetonitrile (4.0 mL) was added 1 N HCl (solution in diethyl ether) (2.13 mL, 2.13 mmol). After the mixture was stirred for 20 min the solvent was evaporated and the residue was azeotroped with toluene to yield ethyl 3-{3-cyano-4-[((2*R*)-3-{[1,1-dimethyl-2-(2-naphthalenyl)-ethyl]amino}-2-hydroxypropyl)oxy]phenyl}propanoate hydrochloride as a white solid (quantitative). ^{1}H NMR (400 MHz, DMSO-d_6): δ 1.16 (s, 3 H) 1.29 (s, 6 H) 2.59−2.65 (m, 2 H), 2.79−2.86 (m, 2 H), 3.13−3.24 (m, 3 H), 3.34−3.44 (m, 1 H), 4.00−4.08 (m, 2 H), 4.15−4.31 (m, 3 H), 5.96−6.01 (m, 1 H), 7.21−7.25 (m, 1 H), 7.37−7.42 (m, 1 H), 7.48−7.59 (m, 3 H), 7.63 (s, 1 H), 7.77−7.80 (m, 1 H), 7.87−7.94 (m, 3 H), 8.60−8.81 (m, 2 H). ^{13}C NMR: δ 14.07, 22.33, 22.41, 28.78, 34.74, 42.68, 43.88, 59.70, 59.84, 65.30, 70.64, 100.55, 113.30, 116.42, 125.86, 126.17, 127.44, 127.59, 129.00,129.22, 131.94, 132.84, 132.88, 133.06, 133.82, 135.10, 158.41, 171.96. LCMS (*m*/*z*): 475.2 $[M+H]^+$. $[\alpha]_D^{20.4}$ +15.43 (*c* 0.77, MeOH). Anal. Calcd for $C_{29}H_{35}N_2O_4Cl \cdot 0.25H_2O$: C, 67.56%, H 6.94%, N 5.43%. Found: C 67.16%, H 6.99%, N 5.33%.

3-{3-Cyano-4-[((2*R*)-3-{[1,1-dimethyl-2-(2-naphthalenyl)ethyl]-amino}-2-hydroxypropyl)oxy]phenyl}propanoic Acid Hydrochloride (12). To a solution ethyl 3-{3-cyano-4-[((2*R*)-3-{[1,1-dimethyl-2-(2-naphthalenyl)ethyl]amino}-2-hydroxypropyl)oxy]phenyl}-propanoate (**11**, 468. 0 mg, 0.987 mmol) in methanol (4.0 mL) was added aqueous 3 N NaOH (0.823 mL, 2.47 mmol). After overnight stirring at room temperature, the solvent was evaporated and the residue was diluted with water (15 mL). The mixture was acidified to pH ∼6 to obtain a solid that was filtered and washed with ethyl ether and acetonitrile. The solid was then

azeotroped with toluene, suspended in acetonitrile, and then treated with 1 N HCl (in ethyl ether) (2.71 mL, 2.71 mmol). The solid product was filtered and washed with a small amount of acetonitrile to yield the title compound (245 mg, 38.4%). ^{1}H NMR (400 MHz, DMSO-d_6): δ 1.29 (s, 6 H), 2.54−2.59 (m, 2 H), 2.77−2.84 (m, 2 H), 3.18 (s, 3 H), 3.36−3.43 (m, 1 H), 4.15−4.30 (m, 3 H), 5.97−6.04 (m, 1 H), 7.24 (d, J = 8.59 Hz, 1 H), 7.39−7.43 (m, 1 H), 7.48−7.59 (m, 3 H), 7.63 (s, 1 H), 7.78 (s, 1 H), 7.87−7.94 (m, 3 H), 8.65−8.72 (m, 1 H), 8.76−8.85 (m, 1 H), 12.15 (s, 1 H). ^{13}C NMR: δ 22.42, 28.86, 34.94, 42.75, 43.89, 54.89, 65.38, 70.64, 100.54, 113.30, 116.46, 125.85, 126.16, 127.44, 127.57, 129.01, 129.21, 131.93, 132.82, 133.01, 134.19, 135.08, 158.35, 173.52. HRMS: 447.2282 (calcd 447.2284). $[\alpha]_D^{23.6}$ +11.75 (c 0.74, DMSO). HPLC purities: method A, 98.5%, t_R = 6.95 min; method C, 100%, t_R = 2.76 min.

Acknowledgment. The authors thank Drs. John Gleason and Brian Metcalf for their support of this work.

References

(1) Bonnick, S. L. Osteoporosis in men and women. *Clin. Cornerstone* **2006**, *8*, 28–39.

(2) Bodenner, D.; Redman, C.; Riggs, A. Teriparatide in the management of osteoporosis. *Clin. Interventions Aging* **2007**, *2*, 499–507. Bilezikian, J. P. Anabolic therepy for osteoporosis. *Women's Health* **2007**, *3*, 243–253. Girotra, M.; Rubin, M. R.; Bilezikian, J. P. The use of parathyroid hormone in the treatment of osteoporosis. *Rev. Endocr. Metab. Disord.* **2006**, *7*, 113–121. Eriksen, E. F.; Robins, D. A. Teriparatide: a bone formation treatment for osteoporosis. *Drugs Today* **2004**, *40*, 935–948. Quattrocchi, E.; Kourlas, H. Teriparaitide: a review. *Clin. Ther.* **2004**, *26*, 841–854. Dobnig, H. A review of teriparatide and its clinical efficacy in the treatment of osteoporosis. *Expert Opin. Pharmacother.* **2003**, *57*, 710–718. Ebling, P. R.; Russell, R. G. G. Teriparaitide (rhPTH1-34) for the treatment of osteoporosis. *Int. J. Clin. Pract.* **2003**, *57*, 710–718. Berg, C.; Neumeyer, K.; Kirkpatrick, P. Fresh from the pipline: teriparatide. *Nat. Rev. Drug Discovery* **2003**, *2*, 257–258.

(3) Brown, E. M.; MacLeod, R. J. Extracellular calcium sensing and extracellular calcium signaling. *Physiol. Rev.* **2001**, *81*, 239–297. Nemeth, E. F. Calcium receptor-dependent regulation of cellular functions. *News Physiol. Sci.* **1995**, *10*, 1–5. Brown, E. M.; MacLeod, R. J. Extracellular calcium sensing and extracellular calcium signaling. *Physiol. Rev.* **2001**, *81*, 239–297. Chen, R. A.; Goodman, W. G. Role of the calcium-sensing receptor in parathyroid gland physiology. *Am. J. Physiol.: Renal Physiol.* **2004**, *286*, F1005–F1011. Tfelt-Hansen, J.; Brown, E. M. The calcium-sensing receptor in normal physiology and pathophysiology: a review. *Crit. Rev. Clin. Lab. Sci.* **2005**, *42*, 35–70.

(4) Locatelli, F.; Pontoriero, G.; Limbardo, M.; Tentori, F. Cinacalcet hydrochloride: calcimimnetic for the treatment of hyperparathyroidism. *Expert Opin. Endocr. Metabol.* **2006**, *1*, 167–179. Dong, B. J. Cinacalcet: an oral calcimimetic agent for the management of hyperparathyroidism. *Clin. Ther.* **2005**, *27*, 1725–1751. de Francisco, A. L. M.; Cinacalcet, H. C. L. A novel therapeutic for the treatment of hyperparathyroidism. *Expert Opin. Pharmacother.* **2005**, *6*, 441–452.

(5) Nemeth, E. F.; Delmar, E. C.; Heaton, W. L.; Miller, M. A.; Lambert, L. D.; Conklin, R. L.; Gowen, M.; Gleason, J. G.; Bhatnagar, P. K.; Fox, J. Calcilytic compounds: potent and selective Ca^{+2} receptor antagonists that stimulate secretion of parathyroid hormone. *J. Pharmacol. Exp. Ther.* **2001**, *299*, 323–331. Gowen, M.; Stroup, G. B.; Dodds, R. A.; James, I. E.; Votta, B. J.; Smith, B. R.; Bhatnagar, P. K.; Lago, A. M.; Callahan, J. F.; Del Mar, E. G.; Miller, M. A.; Nemeth, E. F.; Fox, J. Antagonizing the parathyroid calcium receptor stimulates parathyroid secretion and bone formation in osteopenic rats. *J. Clin. Invest.* **2000**, *105*, 1595–1604. Arey, B. J.; Seethala, R.; Ma, Z.; Fura, A.; Morin, J.; Swartz, J.; Vyas, V.; Yang, W.; Dickson, J. K., Jr.; Feyen, J. H. M. A novel calcium-sensing receptor antagonist transiently stimulates parathyroid hormone secretion in vivo. *Endocrinology* **2005**, *5*, 1131–1136. Dauban, P.; Ferry, S.; Faure, H.; Ruat, M.; Dodd, R. H. N^1-Arylsulfonyl-N^2-(1-aryl)ethyl-3-phenylpropane-1,2-diamines as novel calcimimetics acting on the calcium sensing receptor. *Bioorg. Med. Chem. Lett.* **2000**, *10*, 2001–2004. Kessler, A.; Faure, H.; Ruat, M.; Dauban, P.; Dodd, R. H. N^2-Benzyl-N^1-(1-(1-naphthyl)ethyl)-3-phenylpropane-1,2-diamines and conformationally constrained indole analogues: development of calindol as a new calcimimetic acting at the calcium-sensing receptor. *Bioorg. Med. Chem. Lett.* **2004**, *14*, 3345–3349. Kessler, A.; Faure, H.; Roussanne, M. C.; Ferry, S.; Ruat, M.; Dauben, P.; Dodd, R. H. N^1-Arylsulfonyl-N^2-(1-(1-naphthyl)ethyl)-1,2-diaminocyclohexanes: a new class of calcilytic agents acting at the calcium-sensing receptor. *ChemBioChem* **2004**, *5*, 1131–1136. Arey, B. J.; Seethala, R.; Ma, Z.; Fura, A.; Morin, J.; Swartz, J.; Vyas, V.; Yang, W.; Dickson, J. K., Jr.; Feyen, J. H. M. A novel calcium-sensing receptor antagonist transiently stimulates parathyroid hormone secretion in vivo. *Endocrinology* **2005**, *5*, 1131–1136. Yang, W.; Wang, Y.; Roberge, J. Y.; Ma, Z.; Liu, Y.; Lawerence, R. M.; Rotella, D. P.; Seethala, R.; Feyen, J. H. M.; Dickson, J. K., Jr. Discovery and structure activity relationships of benzylpyrrolidine substituted aryloxypropanols as calcium-sensing receptor antagonists. *Bioorg. Med. Chem. Lett.* **2005**, *15*, 1225–1228. Gavai, A. V.; Vaz, R. J.; Mikkilineni, A. B.; Roberge, J. Y.; Liu, Y.; Lawrence, R. M.; Corte, J. R.; Yang, W.; Bednarz, M.; Dickson, J. K., Jr.; Ma, Z.; Seethala, R.; Feyen, J. H. M. Discovery of novel 1-arylmethyl pyrrolidin-2-yl ethanol amines as calcium-sensing receptor antagonists. *Bioorg. Med. Chem. Lett.* **2005**, *15*, 5478–5482. Shcherbakova, I.; Balandrin, M. F.; Fox, J.; Ghatak, A.; Heaton, W.; Conklin, R. L. 3H-Quinazolin-4-ones as a new calcilytic template for the potential treatment of osteoporosis. *Bioorg. Med. Chem. Lett.* **2005**, *15*, 1557–1560. Shcherbakova, I.; Huang, G.; Geoffroy, O. J.; Nair, S. K.; Swierczek, K.; Balandrin, M. F.; Fox, J.; Heaton, W. L.; Conklin, R. L. *Bioorg. Med. Chem. Lett.* **2005**, *15*, 2537–2540.

(6) Dobnig, H.; Turner, R. T. Evidence that intermittent treatment with parathyroid hormone increases bone formation in adult rats by activation of bone lining cells. *Endocrinology* **1995**, *136*, 3632–3638. Ishizuya, T.; Yokose, S.; Hori, M.; Noda, T.; Suda, T.; Yoshiki, S.; Yamaguchi, A. Parathyroid hormone exerts disparate effects on osteoclast differentiation depending on exposure time in rat osteoblastic cells. *J. Clin. Invest.* **1997**, *99*, 2961–2970. Frolik, C. A.; Black, E. C.; Cain, R. L.; Satterwhite, J. H.; Brown-Augsburger, P. L.; Sato, M.; Hock, J. M. Anabolic and catabolic bone effects of human parathyroid hormone (1−34) are predicted by duration of hormone exposure. *Bone* **2003**, *33*, 372–379. Onyia, J. E.; Helvering, L. M.; Gelbert, L.; Wei, T.; Huang, S.; Chen, P.; Dow, E. R.; Maran, A.; Zhang, M.; Lotinun, S.; Halladay, D. L.; Miles, R. R.; Kulkarni, N. H.; Ambrose, E. M.; Ma, Y. L.; Frolik, C. A.; Sato, M.; Bryant, H. U.; Turner, R. T. Molecular profile of catabolic versus anabolic treatment regimens of parathyroid hormone (PTH) in rat bone: an analysis of DNA microarray. *J. Cell. Biochem.* **2005**, *95*, 403–418.

(7) Marquis, R. W.; Lago, A. M.; Callahan, J. F.; Trout, R. E. L.; Gowen, M.; DelMar, R. G.; Van Vegnan, B. C.; Logan, S.; Shimizu, S.; Fox, J.; Nemeth, E. F.; Yang, Z.; Roethke, T.; Smith, B. R.; Ward, K. W.; Lee, J.; Keenan, R. M.; Bhatnagar, P. Antagonists of the calcium receptor I. Amino alcohol-based parathyroid hormone secretagogues. *J. Med. Chem.* **2009**, *52*, 3982–3993.

(8) Crivori, P.; Poggesi, I. Predictive model for identifying potential CYP2D6 Inhibitors. *Basic Clin. Pharm. Toxicol.* **2005**, *96*, 251–253. Ekins, S.; Gianpaolo, B.; Binkley, S.; Gillespie, J. S.; Ring, B. J.; Winkel, J. H.; Wrighton, S. A. Three and four dimensional-quantitative structure activity relationship (3D/4D-QSAR) analyses of CYP2D6 inhibitors. *Pharmacogenetics* **1999**, *9*, 477–489. De Groot, M. J.; Ackland, M. J.; Horne, V. A.; Alex, A. A.; Jones, B. C. Novel approach to predicting P450-mediated drug metabolism: development of a combined protein and pharmacophore model for CYP2D6. *J. Med. Chem.* **1999**, *42*, 1515–1524. Rowland, P.; Blaney, F. E.; Smyth, M. G.; Jones, J. J.; Leydon, V. R.; Oxbrow, A. K.; Lewis, C. J.; Tennant, M. G.; Modi, S.; Eggleston, D. S.; Chenery, R. J.; Bridges, A. M. Crystal structure of the human cytochrome P450 2D6. *J. Biol. Chem.* **2006**, *281*, 7614–7622. Mitcheson, J. S. hERG potassium channels and the structural basis of drug-induced arrhythmias. *Chem. Res. Toxicol.* **2008**, *21*, 1005–1010. Kramer, C.; Beck, B.; Kriegel, J. M.; Clark, T. A composite model for hERG blockade. *ChemMedChem* **2008**, *3*, 254–265. Stansfeld, P. J.; Gedeck, P.; Gosling, M.; Cox, B.; Mitcheson, J. S.; Sutcliffe, M. J. Drug block of the hERG potassium channel: insights from modeling. *Proteins: Struct., Funct., Bioinf.* **2007**, *68*, 568–580. Sanguinetti, M. C.; Tristani-Firouzi, M. hERG potassium channels and cardiac arrhythmia. *Nature* **2006**, *440*, 463–469. Sanguinetti, M. C.; Mitcheson, J. S. Predicting drug-hERG channel interactions that cause acquired long QT syndrome. *Trends Pharmacol. Sci.* **2005**, *26*, 119–124. Fernandez, D.; Ghanta, A.; Kauffman, G. W.; Sanguinetti, M. C. Physiochemical features of the hERG channel binding site. *J. Biol. Chem.* **2004**, *279*, 10120–10127. Tonioli, C.; Crisma, M.; Formaggio, F.; Peggion, C. Control of peptide conformation by the Thorpe−Ingold effect (C-α tetrasubstitution). *Biopolymers* **2001**, *60*, 396–419.

(9) See first two references of ref 6.